Journal of Solid State Chemistry **152,** 381–387 (2000)
doi:10.1006/jssc.2000.8666, available online at http://www.idealibrary.com on IDEAL®

# Preparation and Crystal Structures of $Ni(NH_3)_2Cl_2$ and of Two Modifications of $Ni(NH_3)_2Br_2$ and $Ni(NH_3)_2I_2$

A. Leineweber[1] and H. Jacobs

*Lehrstuhl Anorganische Chemie I, Fachbereich Chemie der Universität, 44221 Dortmund, Germany*

Received December 15, 1999; accepted February 24, 2000

**Diammine nickel(II) halides, $Ni(NH_3)_2X_2$ ($X$ = Cl, Br, I), were prepared by decomposition of the corresponding hexaammines at 120°C in dynamical vacuum. Their crystal structures are of the $Cd(NH_3)_2Cl_2$ type ("$\beta$-type", space group *Cmmm*, $Z = 2$): for $Ni(NH_3)_2Cl_2$, $a = 8.019$ Å, $b = 8.013$ Å, $c = 3.661$ Å; for $\beta$-$Ni(NH_3)_2Br_2$, $a = 8.273$ Å, $b = 8.297$ Å, $c = 3.851$ Å. Both were obtained by Rietveld refinement of diffractometer data with standard deviations < 0.001 Å. For $\beta$-$Ni(NH_3)_2I_2$, $a = b = 8.753(3)$ Å, $c = 4.127(1)$ Å, obtained by Guinier film data. In the case of the bromide and the iodide, annealing at 300°C leads to an irreversible structural rearrangement. A new modification is formed which is of the $Mg(NH_3)_2Br_2$ type ("α-type", space group *Pbam*, $Z = 2$): for α-$Ni(NH_3)_2Br_2$, $a = 5.865$ Å, $b = 11.723$ Å, $c = 3.856$ Å, obtained by Rietveld refinement of diffractometer data with standard deviations < 0.001; for α-$Ni(NH_3)_2I_2$, $2a = b = 12.359(3)$ Å, $c = 4.126(1)$ Å, obtained by Guinier film data. Both types of structures contain infinite chains of edge-sharing octahedra $^1_\infty[NiX_{4/2}(NH_3)_2]$. These run parallel to the *c*-axes of the unit cells of the corresponding structure types and are arranged in different ways relative to one another. The decomposition of hexaammine nickel(II) halides to the corresponding diammines is analyzed in terms of structural analogies.** 

***Key Words:*** **diammines of metal(II) halides; ammoniates of nickel halides; polymorphism of metal diammine halides; dynamical disorder of ammonia ligands; Rietveld refinement; structural analogue's between ammoniates.**

## INTRODUCTION

Ammines of simple salts $M(NH_3)_nX_m$ are of interest for several reasons. They can serve as model systems for a stepwise solvation of salts. For example, this was systematically examined on the crystal structures of a series of ammines $Al(NH_3)_nCl_3$ with $n = 1, 2, 3, 5, 6$ (1–3). Furthermore, there is fundamental interest in the rotational dynamics of the $NH_3$ molecules fixed by coordinative bonds to metal centers. Often this is accompanied by order–disorder transformations (e.g., in hexaammine metal(II) halides (4)). With respect to the last point, the role of hydrogen bonds in ammines was examined (e.g., (5, 6)). Additionally, ammines may be used as precursors for crystal growth of nitrides in supercritical ammonia (e.g., $Cu_3N$ (7), $Cu_3PdN$ (8), or $\eta$-$Mn_3N_2$ (9)).

At the beginning of the 20th century thermodynamic studies were carried out on several systems $M(NH_3)_nX_m$ in order to determine the different values of $n$ and the corresponding $NH_3$ pressures $p(n, T)$. Many results of these works are reported in (10).

For the ammines of $M$ = Mg, Mn, Fe, Co, Ni (with $m = 2$) and $X$ = Cl, Br, I strong analogies were found. The different systems show similarities in solvation numbers of $n \leq 6$ with $n = 1, 2, 6$ for $X$ = Cl, Br and $n = 2, 6$ for $X = I$ (10). Ammines with $n > 6$ are only stable below ambient temperatures (10) and are not of interest here.

The structures of the hexaammines $M(NH_3)_6X_2$ were thoroughly examined by X-ray (11–13) and neutron diffraction methods (14). They are built up by $[M(NH_3)_6]^{2+}$ and $X^-$ ions arranged with the motif of the cubic $CaF_2$ type (at ambient temperatures $Fm\bar{3}m$ with disordered H atoms (12–14)). The hexaammines can in many cases be crystallized from aqueous ammonia solutions. This is not possible for the ammines with a lower $n$. This causes difficulties for the preparation of well-crystallized materials.

We had started structural investigations of ammines of lower $NH_3$ content to examine the diammine halides of magnesium, $Mg(NH_3)_2X_2$ ($X$ = Cl, Br, I) (15). In this study we have found the $Cd(NH_3)_2Cl_2$ structure type (*Cmmm*) (16) for the chloride and established the then unprecedented $Mg(NH_3)_2Br_2$ structure type (*Pbam*) for the bromide and iodide. Both structure types contain parallel chains $^1_\infty[MX_{4/2}(NH_3)_2]$ of edge-sharing octahedra, which are arranged in different ways relative to one another (Fig. 1). For the bromide and the iodide single crystals were grown by reaction of magnesium with the corresponding ammonium halide.

Now, we have extended our studies to the systems $NiX_2/NH_3$ ($X$ = Cl, Br, I). These ammines have already

[1]Present address: MPI für metallforschung, seestraße 92, D-70174 Stuttgart, Germany.



0022-4596/00 $35.00

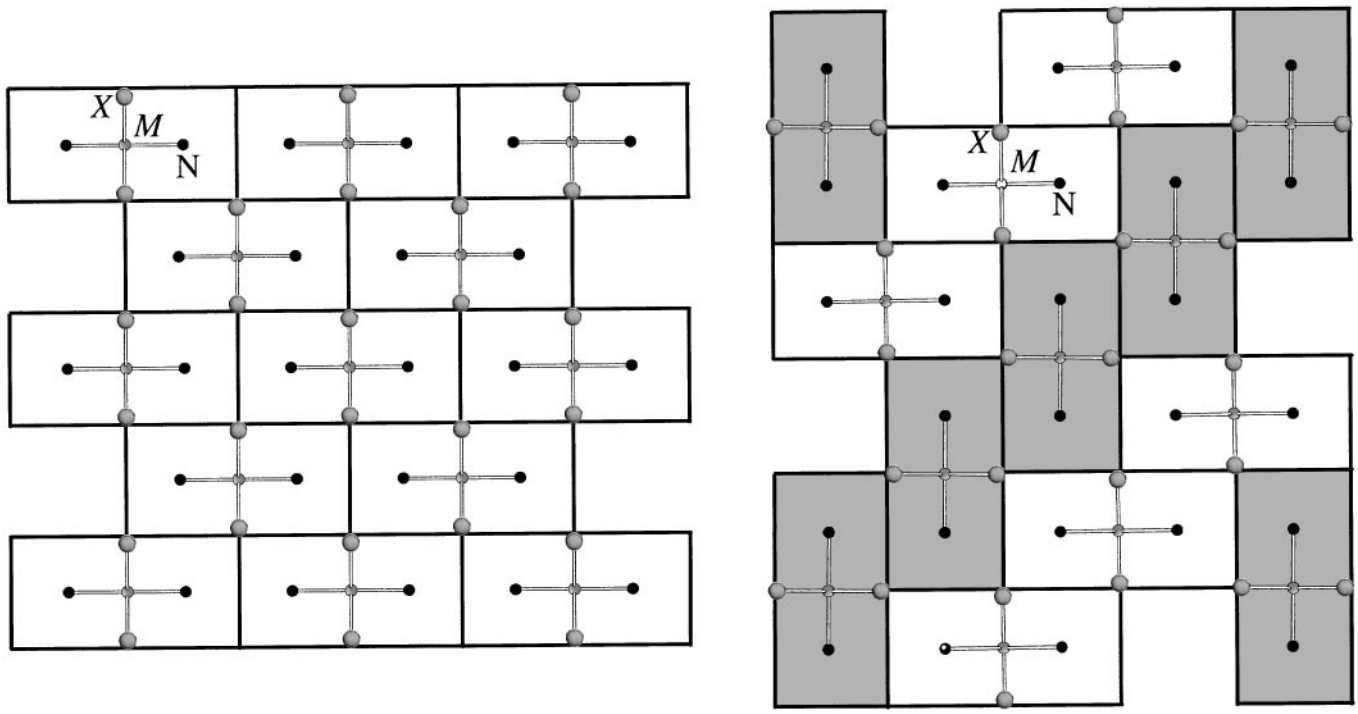


**FIG. 1.** Schematic representation of the $Cd(NH_3)_2Cl_2$ and the $Mg(NH_3)_2Br_2$ type structures in a (001) projection. Chains $^1_\infty[MX_{4/2}(NH_3)_2]$ run parallel to the *c*-axis. The subdivision into square units shows the relation to a CsCl type arrangement of *X* and *N*. "Double CsCl cells" are indicated as units, in which one $^1_\infty[MX_{4/2}(NH_3)_2]$ unit is located.

been reported in (17, 18) including determinations of the $NH_3$ absorption isotherms.

X-ray powder diffraction data on the diammine chloride are given in (19). A tetragonal primitive unit cell ($a = 5.60$ Å, $c = 3.70$ Å) is reported and "similarity" of the crystal structure of $Ni(NH_3)_2Cl_2$ to the $Cd(NH_3)_2Cl_2$ type (16) is suggested. Further support for this assumption comes from the fact that $Ni(H_2O)_2Cl_2$ (20, 21) forms a slightly distorted (due to hydrogen bonding) variant of the $Cd(NH_3)_2Cl_2$ structure type. This was already pointed out in (22). However, no rigorous structural analysis of the crystal structure of $Ni(NH_3)_2Cl_2$ has been reported until now.

In (23) the structures of $Ni(NH_3)_2Cl_2$ and $Ni(NH_3)_2Br_2$ were reported to be probably isotypic and powder patterns were indexed with a tetragonal primitive unit cell ($a = 5.66$ Å, $c = 3.66$ Å for the chloride; $a = 5.86$ Å, $c = 3.85$ Å for the bromide).

For $Ni(NH_3)_2I_2$ again chains of $^1_\infty[NiI_{4/2}(NH_3)_2]$ were suggested to constitute the structure (24). This was deduced from a small magnetic transition entropy (antiferromagnetic–paramagnetic) which supports a low dimensionality of magnetic interactions. Powder diffraction patterns were indexed with an orthorhombic unit cell ($a = 12.38$ Å, $b = 13.17$ Å, and $c = 8.28$ Å). However, the proposed structural elements were not related to the cell parameters.

UV spectroscopic investigations of diammine nickel(II) chloride and bromide confirm octahedral coordination of Ni (e.g., (25)). IR spectroscopy was performed on the chloride (5) and hydrogen bonding was analyzed.

We will now report optimized methods of preparation and elucidation of the structures of one modification of diammine nickel(II) chloride and of two modifications each of diammine nickel(II) bromide and iodide.

## PREPARATION

All diammines are sensitive to moist air and were handled under inert conditions (26). Furthermore, the hexaammines show slow exchange of $NH_3$ by $H_2O$ indicated by a change of color from deep blue to green. This is prevented by keeping the materials in closed containers. The sensitivity to moist air is most pronounced for the chloride. Its equilibrium $NH_3$ pressure is the highest (17, 18).

The method described for the growth of single crystals of diammine magnesium halides in (15) was not successful for the nickel compounds; nickel powder does not react with $NH_4X$ ($X$ = Cl, Br, I) at 350°C in autoclaves.

Therefore, first $Ni(NH_3)_6X_2$ ($X$ = Cl, Br) was prepared by introducing $NH_3$ gas (99.999%, Messer-Griesheim) into a saturated aqueous solution of $NiCl_2 \cdot 6H_2O$ (purity >97%, Merck) or $NiBr_2$ (99%, Aldrich) along with some $NH_4Cl$

(>99.8%, Merck) or $NH_4Br$ (>99%, Aldrich). The hexaammines crystallize from these solutions on slow cooling.

$Ni(NH_3)_6I_2$ was prepared from a 1:2 (molar ratio) aqueous solution of $NiSO_4 \cdot 6\ H_2O$ (99%, Aldrich) and $NH_4I$ (> 99.8%, Merck) by introduction of $NH_3$ gas. The crystalline product precipitates readily from the solution.

The hexaammine materials were gathered on a glass filter crucible. It was first washed with an aqueous solution of $NH_3/NH_4Cl$ (each 0.5 molar) and then with EtOH saturated with gaseous ammonia.

Second, hexaammine nickel(II) chloride was placed into a glass tube attached to dynamic vacuum ($p < 0.1$ Torr). The tube was slowly heated by an oil bath, finally reaching 120°C. The material changed its color from the initial blue to light green.

If the temperature is increased too fast, the evolution of $NH_3$ gas can occur vigorously. A glass fritted disc prevented the contamination of the vacuum line with the fine powder and helped to keep the decomposition reaction under control. The final product was a light green very fine powder. It was annealed in a steel autoclave for 2 days at 300°C in order to improve crystallinity. The autoclave ($V = 7$ ml) was filled and closed under an argon atmosphere at ambient pressures. At elevated temperatures a small amount of the ammine decomposes to build up its equilibrium $NH_3$ pressure (about 600 Torr at 300°C (17)) to prevent further decomposition.

The procedure for the preparation of $Ni(NH_3)_2X_2$ ($X$ = Br, I) was the same as that for the diammine chloride: The decomposition reaction with $T_{max} = 120$°C gave $\beta$-$Ni(NH_3)_2X_2$. Annealing of these products at 300°C as described for the diammine chloride led, for both the bromide and the iodide, to an irreversible transformation into $\alpha$-$Ni(NH_3)_2X_2$ as revealed by powder diffraction patterns. The bromide is yellowish green, the iodide orange brown. The colors appeared brighter after annealing.

Annealing experiments ($t = 24$ h) on $\beta$-$Ni(NH_3)_2Br_2$ as a function of temperature (175°C < $T$ < 300°C, intervals of 25°C) were performed in glass ampoules under an argon atmosphere.

## X-RAY INVESTIGATIONS AND RIETVELD REFINEMENT

Guinier patterns were taken from all products on an FR552 camera (Cu$K\alpha_1$ radiation, Enraf-Nonius, Delft, The Netherlands). Si was used as an internal standard.

X-ray powder diffractograms were taken from flat samples (thickness $\approx 1$ mm) covered by Kapton foil ($d \approx 50$ μm, type 200 HN, August Krempel Söhne GmbH & Co., Enzweihingen, Germany) on a Siemens D500 powder diffractometer (Cu$K\alpha$ radiation, Bragg-Brentano geometry, graphite as secondary monochromator).

Samples of $Ni(NH_3)_2Cl_2$ after thermal decomposition of the hexaammine at 120°C as well as after annealing at 300°C showed the same reflections. However, the thermal treatment leads to a significant narrowing of the reflections.

A powder diffraction pattern was taken from the annealed material. It is similar to the tetragonally indexed pattern reported in (19). A C-centered orthorhombic $Cd(NH_3)_2Cl_2$ structure type (16) was used as a starting model for the Rietveld refinement (27). For this model the unit cell dimensions are roughly $2^{1/2} \times 2^{1/2} \times 1$ larger than the cell proposed in (19). The increased cell size does not require new reflections as a result of the C-centering but allows a splitting of the positions of certain reflections. This was in fact observed in the case of $Mg(NH_3)_2Cl_2$ for well-resolved Guinier patterns (15), but not for $Ni(NH_3)_2Cl_2$. The Rietveld refinement readily converged. A preferred orientation according to the [001] direction as an ellipsoid (March– Dollase model (28, 29)) had to be considered. This direction corresponds to that of the $^1_\infty[NiCl_{4/2}(NH_3)_2]$ chains.

The scattering power of hydrogen is significant in this compound. A refinement without taking H into account leads to negative thermal parameters of N and to worse residuals. Indeed, the contribution of H is due to integral scattering of the whole $NH_3$ molecule whereas a superstructure due to a specific orientational ordering of $NH_3$ would cause only very weak new reflections. Most probably, the $NH_3$ molecules are rotationally disordered at ambient temperatures, as is known for the hexaammines (12–14). This is in accordance with the evaluation of first neutron diffraction data on $Co(ND_3)_2Cl_2$ ($\beta$-type modification) and $Mg(ND_3)_2Br_2$ (30). In most of the above-mentioned cases the hydrogen density distribution can approximately be described by four maxima pointing to the four halogen atoms next to the $NH_3$ group. We introduced the H positions for all our refinements. They were modeled by soft constraints to form a square with edges of 1.1 Å and a distance N–H of 0.85 Å, each site with an occupancy of 3/4 and a thermal displacement parameter $U(H) = 2U(N)$.

Details of data collection and Rietveld refinement for the data of $Ni(NH_3)_2Cl_2$ are given in Table 1, the final structural parameters in Table 2, and selected atomic distances and angles in Table 3. The diffraction data, the fitted profile, and the difference curve are displayed in Fig. 2.

Figure 3 shows a zoom of the range $10° < 2\theta < 45°$ of the diffraction data for $\beta$- and $\alpha$-$Ni(NH_3)_2Br_2$, i.e., before and after annealing. The thermal treatment leads to a considerable narrowing of the reflection profiles and to additional reflections. Slow cooling after the annealing shows that the transition is monotropic.

In analogy to $Ni(NH_3)_2Cl_2$ the powder diffractograms of the $\beta$-modification of $Ni(NH_3)_2Br_2$ can be refined on the basis of a $Cd(NH_3)_2Cl_2$ type model whereas the patterns of the $\alpha$-modification fit to an $Mg(NH_3)_2Br_2$ type structure. H-atoms were introduced fixed to N as mentioned above. For

**TABLE 1**
**Details of X-Ray Powder Diffractometry and Subsequent Rietveld Refinement for Diammine Nickel(II) Halides**

| | | | |
|---|---|---|---|
| Formula | $Ni(NH_3)_2Cl_2$ | $\beta$-$Ni(NH_3)_2Br_2$ | $\alpha$-$Ni(NH_3)_2Br_2$ |
| Formula weight | 163.7 | 252.6 | 252.6 |
| Diffractometer | Siemens D500, Bragg Brentano | | |
| Radiation | Cu$K\alpha$ (Graphite secondary monochromator) | | |
| $2\theta$ range | 10–120° | | |
| $2\theta$ step width | 0.01° | | |
| Time per step | 5 s | | |
| Space group | *Cmmm* (No. 65) | | *Pbam* (No. 55) |
| Cell parameters[b] $a$ in Å | 8.019 | 8.273 | 5.865 |
| $b$ in Å | 8.013 | 8.297 | 11.723 |
| $c$ in Å | 3.661 | 3.851 | 3.856 |
| Volume $V$ in Å$^3$, $Z$ | 235.2, 2 | 264.3, 2 | 265.1, 2 |
| Calculated density in g/cm$^3$ | 2.31 | 3.17 | 3.16 |
| Profile parameters | 4 | 4 | 4 |
| Background parameters | 8 + 7 fixed background | 8 + 8 fixed background | 6 + 8 fixed background |
| Structural parameters | 5 | 5 | 7 |
| Zero point in ° | − 0.0247(6) | − 0.057(2) | 0.0313(6) |
| Preferred orientation parameter $r$ according to (28, 29) | 0.940(2) | 0.874(2) | — |
| No. of reflections | 248 | 306 | 472 |
| w$R_P$ | 8.0 | 7.1 | 8.5 |
| $R(F^2)$ ($F^2 \geq \sigma(F^2)$) | 8.9 | 9.7 | 8.9 |

[a] Simpson's rule integration of Pseudovoigt function with correction for asymmetry (34, 35).
[b] Standard deviations resulting from Rietveld refinements are smaller than 0.001 Å.

the $\beta$-modification we again had to consider preferred orientation as described above for $Ni(NH_3)_2Cl_2$ again using the direction [001] as ellipsoid axis. For $\alpha$-$Ni(NH_3)_2Br_2$ an analogous attempt does not improve the residuals significantly.

Details of the Rietveld refinements are given in Table 1. The final structural parameters are given in Tables 2 and 4. In Figs. 4 and 5 we present the final profile fits of both modifications of $Ni(NH_3)_2Br_2$. Selected atomic distances are given in Table 3.

**TABLE 2**
**Refined Positional and Thermal Parameters of $Ni(NH_3)_2Cl_2$ and $\beta$-$Ni(NH_3)_2Br_2$ (*Cmmm*)**

| Atom | Wyckoff site | $x$ | $y$ | $z$ | $f_{occ}$ | 100 $U_{iso}$/Å$^2$ |
|---|---|---|---|---|---|---|
| | | | $Ni(NH_3)_2Cl_2$ | | | |
| Ni | 2*a* | 0 | 0 | 0 | 1 | 1.13(7) |
| Cl | 4*h* | 0.2148(2) | 0 | 1/2 | 1 | 0.7(1) |
| N | 4*i* | 0 | 0.2608(4) | 0 | 1 | 0.91(6) |
| H[a] | 16*r* | 0.069 | 0.303 | 0.150 | 3/4 | 2 $U$(N) |
| | | | $\beta$-$Ni(NH_3)_2Br_2$ | | | |
| Ni | 2*a* | 0 | 0 | 0 | 1 | 3.7(1) |
| Br | 4*h* | 0.2271(2) | 0 | 1/2 | 1 | 1.81(6) |
| N | 4*i* | 0 | 0.2520(8) | 0 | 1 | 4.2(2) |
| H[a] | 16*r* | 0.067 | 0.294 | 0.143 | 3/4 | 2 $U$(N) |

[a] Constraints: see text.

The diffraction patterns of the iodides are similar to those of the bromides. We did not perform extended powder diffractometer studies. We only determined the unit cell parameters from Guinier patterns. For both modifications pseudo-tetragonal axes were used for a refinement of lattice parameters resulting in $a_t = 12.359(3)$ Å and $c = 4.126(1)$ Å for $\alpha$-$Ni(NH_3)_2I_2$ ($a_o = a_t/2$, $b_o = a_t$) as well as $a_t = 8.735(3)$ Å and $c = 4.127(1)$ Å for $\beta$-$Ni(NH_3)_2I_2$ ($a_o = b_o = a_t$).

Samples of $\beta$-$Ni(NH_3)_2Br_2$ annealed for 24 h at certain temperatures were analyzed by Guinier film methods. For temperatures of $T \leq 200$°C no changes of the $\beta$-phase patterns were observed. At 225°C a pronounced narrowing of the reflections of the $\beta$-phase occurred, while a new broad reflection at $2\theta = 16.5°$ appeared. This has to be assigned to the $\alpha$-phase which has been formed partially. With increasing temperatures, this reflection becomes more intense. At 300°C the transformation seems to be complete: the reflection at $2\theta = 16.5°$ is now as sharp as the others. The patterns do not change by prolonged annealing which indicates a complete transformation of the $\beta$- into the $\alpha$-phase.

**TABLE 3**
**Selected Distances and Angles**

| Distances/Angles | $Ni(NH_3)_2Cl_2$ | $\beta$-$Ni(NH_3)_2Br_2$ | $\alpha$-$Ni(NH_3)_2Br_2$ |
|---|---|---|---|
| 4 × Ni–$X$/Å | 2.513(1) | 2.690(1) | 2.656(1) |
| 2 × Ni–N/Å | 2.089(3) | 2.091(6) | 2.044(5) |
| Bridging $X$–Ni–$X$/° | 86.51(1) | 88.59(4) | 86.89(2) |

**TABLE 4**
**Refined Positional and Thermal Parameters of α-$Ni(NH_3)_2Br_2$ (*Pbam*)**

| Atom | Wyckoff site | *x* | *y* | *z* | $f_{occ}$ | 100 $U_{iso}/Å^2$ |
|---|---|---|---|---|---|---|
| Ni | 2*a* | 0 | 0 | 0 | 1 | 1.89(6) |
| Br | 4*h* | 0.2810(1) | 0.38925(7) | 1/2 | 1 | 1.25(3) |
| N | 4*g* | 0.2479(9) | 0.1226(5) | 0 | 1 | 2.9(1) |
| H(1)[a] | 8*i* | 0.355 | 0.109 | 0.143 | 3/4 | 2 *U*(N) |
| H(2)[a] | 8*i* | 0.225 | 0.177 | 0.143 | 3/4 | 2 *U*(N) |

[a] Constraints: see text.

However, it is difficult to prove the absence of the β-$Ni(NH_3)_2Br_2$ from considering only the positions of reflections. All positions of reflections of the α-phase include also those of the β-phase. However, α-$Ni(NH_3)_2Br_2$ produced from the β-material by annealing for 2 days at 300°C shows no discrepancies in the Rietveld refinement (see above). This may indicate the absence of residual β-$Ni(NH_3)_2Br_2$.

## DISCUSSION

The crystal structures of the diammine nickel(II) halides annealed at 300°C are isotypic to those reported previously for the corresponding diammine magnesium halides (15): the chloride crystallizes in the $Cd(NH_3)_2Cl_2$ type (16) and the bromide as well as the iodide in the $Mg(NH_3)_2Br_2$ type (15). This tendency seems to hold for the corresponding compounds of Mn, Fe, and Co, too (30).

However, the diammine nickel(II) bromide and iodide form a metastable β-modification of the $Cd(NH_3)_2Cl_2$ type after decomposition of the corresponding hexaammine nickel(II) halides at 120°C.

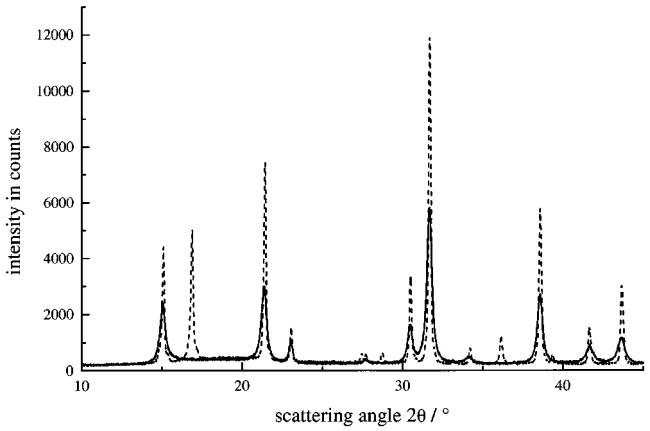


**FIG. 3.** Comparison of the $2\theta = 10–45°$ range of the powder diffraction patterns of α- (- - -) and β-$Ni(NH_3)_2Br_2$ (—).

A comparison of the diffraction patterns of the two modifications of $Ni(NH_3)_2Br_2$ (Fig. 3) indicates that the α-phase may be a superstructure of the β-modification. Figure 6 shows a "tree" of space groups according to (31, 32). The space groups of the $Cd(NH_3)_2Cl_2$ and $Mg(NH_3)_2Br_2$ types of structures are derived from a CsCl type. Figure 6 displays the successive group–subgroup relations. The two structures are located in different branches of the tree. The α-structure is not a superstructure of β-form. The similarity of the diffraction patterns is mainly caused by the unit cell dimensions. These are in both cases close to tetragonal.

The transition of β-$Ni(NH_3)_2Br_2$ into α-$Ni(NH_3)_2Br_2$ seems to be sluggish or of very low energy. We failed to monitor the phase transformation by DSC methods (Pyris 1, Perkin Elmer) with samples in sealed Al crucibles.

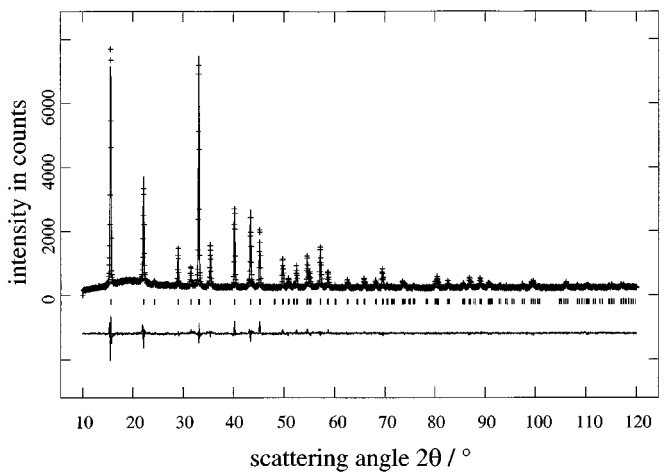


**FIG. 2.** Powder diffraction pattern and results of Rietveld refinement of $Ni(NH_3)_2Cl_2$: +, observed profiles points; —, calculated profile; bottom, difference curve, markers indicate reflection positions.

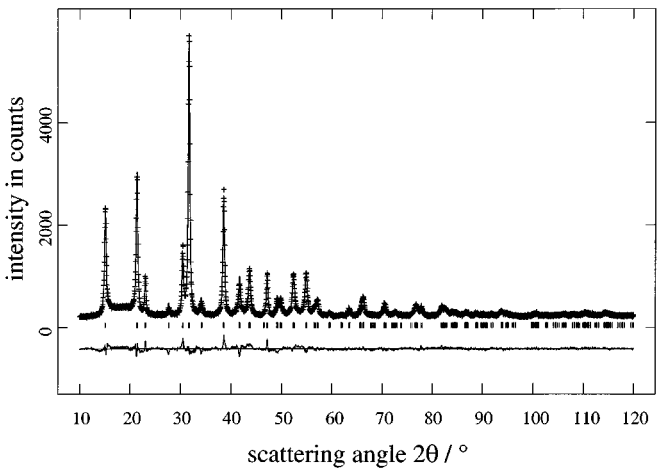


**FIG. 4.** Powder diffraction pattern and results of Rietveld refinement of β-$Ni(NH_3)_2Br_2$: +, Observed profiles points; —, calculated profile; bottom, difference curve, markers indicate reflection positions.

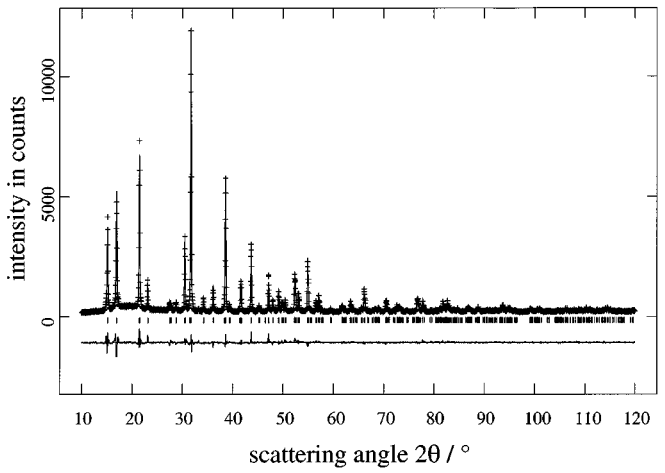


**FIG. 5.** Powder diffraction pattern and results of Rietveld refinement of $\alpha$-$Ni(NH_3)_2Br_2$: +, observed profiles points; —, calculated profile; bottom, difference curve, markers indicate reflection positions.

In order to analyze structural aspects of the observed phase transformation $Ni(NH_3)_6X_2$–$4NH_3 \rightarrow \beta$-$Ni(NH_3)_2X_2 \rightarrow \alpha$-$Ni(NH_3)_2X_2$ (the last step is observed only for $X$ = Br, I) one has to consider the presence of an approximate or exact cubic primitive array of $X$ in all the relevant crystal structures. The hexaammines form an anti-$CaF_2$-like (or anti-$K_2PtCl_6$ type) arrangement with $[Ni(NH_3)_6]^{2+}$ cations occupying half of the cubic interstices formed by $X$. The removal of two-thirds of the $NH_3$ molecules coordinating Ni leads to four free coordination sites. These are saturated for the linear $Ni(NH_3)_2^{2+}$ units by going into a square of $X$. This is reached in such a way that one $NH_3$ molecule is located in each cubic interstitial site. This leads to the image of a CsCl type structure formed by $X$ and $NH_3$ groups. Each metal atom connects two $NH_3$ molecules of two CsCl cells to double units (Fig. 1). The $\alpha$- and the $\beta$-modification are different variants of such a structure, in which all the double cells are located perpendicular to one crystallographic axis leading the $^1_\infty[NiX_{4/2}(NH_3)_2]$ chains. A disordered arrangement of $Hg(NH_3)_2^{2+}$ units in a cubic array of Cl is known for $Hg(NH_3)_2Cl_2$ (16) with a cubic primitive unit cell of the dimension of an CsCl cell and with a statistical distribution of Hg.

The initial formation of the $\beta$-modification by removing $NH_3$ at low temperatures from $Ni(NH_3)_6^{2+}$ indicates that the decomposition of the $Ni(NH_3)_6X_2$ crystals is kinetically controlled. The transformation $\beta$-$Ni(NH_3)_2X_2 \rightarrow \alpha$-$Ni(NH_3)_2X_2$ may be understood as a rearrangement of $Ni(NH_3)_2^{2+}$ units maintaining the array of $X$. However, the transition can also be accomplished by a rotation of half of the $^1_\infty[NiX_{4/2}(NH_3)_2]$ chains by 90°. Further investigations are needed to analyze the mechanism of this transformation.

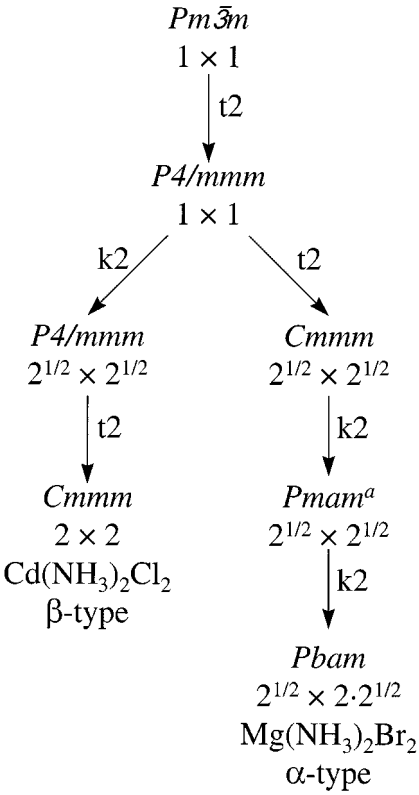


**FIG. 6.** Tree of group–subgroup relationship. Space groups that lead to the $Cd(NH_3)_2Cl_2$ and the $Mg(NH_3)_2Br_2$ type starting from $Pm\bar{3}m$ of an undistorted CsCl type structure are given. $NH_3$ and $X$ play the role of Cs and Cl. The size of the unit cell within the $a,b$-plane is given with respect to the parent CsCl cell. The $c$-axis is the same for all relevant space groups. k2 and t2 denote *klassengleich* and *translationengleich* relations of index 2 between the corresponding groups. This figure shows that the $Cd(NH_3)_2Cl_2$ and the $Mg(NH_3)_2Br_2$ type structures are not derived from one another in the sense of a group–subgroup relationship.

A comparison of the interatomic distances for $\alpha$- and $\beta$-$Ni(NH_3)_2Br_2$ shows differences. However, standard deviations of Rietveld refinements are generally underestimated (33). An especially severe overlap of broad reflections and poor signal-to-noise ratio in the $\beta$-$Ni(NH_3)_2Br_2$ diffraction data enforce a critical evaluation of the resulting structural parameters.

The refined preferred orientation parameters for $Ni(NH_3)_2Cl_2$ and $\beta$-$Ni(NH_3)_2Br_2$ (see Table 1) indicate a plate-like shape of the crystals which is contrary to what is expected from the chain structure. However, this may originate from the specific conditions for the growth of the crystallites from the $Ni(NH_3)_6X_2$ crystals.

## ACKNOWLEDGMENTS

We thank the Fonds der Chemischen Industrie, the Deutsche Forschungsgemeinschaft, and the Bundesministerium für Bildung, Wissenschaft, Forschung und Technologie (JA4DOR) for financial support of this work.

## REFERENCES


1. H. Jacobs and B. Nöcker, *Z. Anorg. Allg. Chem.* **614,** 25 (1992).
2. H. Jacobs and B. Nöcker, *Z. Anorg. Allg. Chem.* **619,** 73 (1993).
3. B. Nöcker, Ph.D. thesis, Universität Dortmund, 1991.
4. L. Asch, G. K. Senoy, J. M. Friedt, J. P. Adloff, and R. Kleinberger, *J. Chem. Phys.* **62,** 2335 (1975).
5. R. Eßmann and Ch. Mockenhaupt, *Spectrochim. Acta A* **52,** 1897 (1996).
6. R. Eßmann, *J. Mol. Struct.* **351,** 91 (1995).
7. H. Jacobs and U. Zachwieja, *J. Less-Common Met.* **161,** 175 (1990).
8. H. Jacobs and U. Zachwieja, *J. Less-Common Met.* **170,** 185 (1991).
9. H. Jacobs and C. Stüve, *J. Less-Common Metals* **96,** 323 (1984).
10. J. Jander, "Anorganische und allgemeine Chemie in flüssigem Ammoniak," Band I, Teilband 1 der Reihe Chemie in nichtwäßrigen ionisierenden Lösungsmitteln, Friedr. Vieweg & Sohn, Braunschweig (1966).
11. I. Olovson, *Acta Crystallogr.* **18,** 889 (1965).
12. H. Jacobs, J. Bock, and C. Stüve, *J. Less-Common Met.* **134,** 207 (1987).
13. R. Eßmann, G. Kreiner, A. Niemann, D. Rechenbach, A. Schmieding, T. Sichla, U. Zachwieja, and H. Jacobs, *Z. Anorg. Allg. Chem.* **622,** 1161 (1996).
14. P. Schiebel, A. Hoser, W. Prandl, G. Heger, W. Paulus, and P. Schweiss, *J. Phys.: Condens. Matter* **6,** 10989 (1994).
15. A. Leineweber, M. W. Friedriszik, and H. Jacobs, *J. Solid State Chem.* **147,** 229 (1999).
16. H. MacGillavry and J. M. Bijvoet, *Z. Kristallogr.* **94,** 249 (1936).
17. W. Biltz and B. Fetkenheuer, *Z. Anorg. Allg. Chem.* **83,** 163 (1913).
18. W. Biltz and B. Fetkenheuer, *Z. Anorg. Allg. Chem.* **89,** 134 (1914).
19. R.-G. Lucas, Ph.D. thesis, Universität Bonn, 1954.
20. B. K. Vainshtein, *Zh. Fiz. Khim.* **26,** 1774 (1952).
21. B. Morosin, *Acta Crystallogr.* **23,** 630 (1967).
22. M. A. Porai-Koshits, *Russ. J. Inorg. Chem.* (Engl. Transl.) **4,** 332 (1959).
23. C. Mockenhaupt and R. Eßmann, 8. Vortragstagung der Fachgruppe Festkörperchemie der GDCh Darmstadt (book of abstracts) (1996), PIII 32.
24. R. D. Worswick, J. C. Cowell, and L. A. K. Staveley, *J. Chem. Soc., Faraday Trans.* 1590 (1974).
25. R. L. Chiang and R. S. Drago, *Inorg. Chem.* **10,** 453 (1971).
26. H. Jacobs and D. Schmidt, *Curr. Top. Mater. Sci.* **8,** 379 (1982).
27. A. C. Larson and R. B. von Dreele, General Structure Determination System (GSAS), Los Alamos National Laboratory, Los Alamos, 1995.
28. A. March, *Z. Kristallogr.* **81,** 285 (1932).
29. W. A. Dollase, *J. Appl. Crystallogr.* **19,** 267 (1986).
30. A. Leineweber, M. W. Friedriszik, H. Jacobs, R. Eßmann, G. Böttger, F. Fauth, and P. Fischer, *Z. Kristallogr. Suppl.* **16,** 46 (1999).
31. H. Bärnighausen, *MATCH* **9,** 139 (1980).
32. Th. Hahn, "International Tables for Crystallography, Vol. A, Space Group Symmetry," Kluwer Academic Publishers, Dordrecht, 1995.
33. R. A. Young, "The Rietveld Method," Oxford Univ. Press, Oxford, 1993.
34. C. J. Howard, *J. Appl. Crystallogr.* **15,** 615 (1982).
35. P. Thomson and J. B. Hastings, *J. Appl. Crystallogr.* **20,** 79 (1987).